Glucokinase Inactivation Paradoxically Ameliorates Glucose Intolerance by Increasing β-Cell Mass in *db/db* Mice

Kazuno Omori,[1] Akinobu Nakamura,[1] Hideaki Miyoshi,[2] Yuki Yamauchi,[1] Shinichiro Kawata,[1] Kiyohiko Takahashi,[1] Naoyuki Kitao,[1] Hiroshi Nomoto,[1] Hiraku Kameda,[1] Kyu Yong Cho,[1,3] Yasuo Terauchi,[4] and Tatsuya Atsumi[1]

Diabetes 2021;70:917–931 | https://doi.org/10.2337/db20-0881

Efficacy of glucokinase activation on glycemic control is limited to a short-term period. One reason might be related to excess glucose signaling by glucokinase activation toward β-cells. In this study, we investigated the effect of glucokinase haploinsufficiency on glucose tolerance as well as β-cell function and mass using a mouse model of type 2 diabetes. Our results showed that in *db/db* mice with glucokinase haploinsufficiency, glucose tolerance was ameliorated by augmented insulin secretion associated with the increase in β-cell mass when compared with *db/db* mice. Gene expression profiling and immunohistochemical and metabolomic analyses revealed that glucokinase haploinsufficiency in the islets of *db/db* mice was associated with lower expression of stress-related genes, greater expression of transcription factors involved in the maintenance and maturation of β-cell function, less mitochondrial damage, and a superior metabolic pattern. These effects of glucokinase haploinsufficiency could preserve β-cell mass under diabetic conditions. These findings verified our hypothesis that optimizing excess glucose signaling in β-cells by inhibiting glucokinase could prevent β-cell insufficiency, leading to improving glucose tolerance in diabetes status by preserving β-cell mass. Therefore, glucokinase inactivation in β-cells, paradoxically, could be a potential strategy for the treatment of type 2 diabetes.

The number of people worldwide with diabetes is almost half a billion and it is predicted to increase 25% by 2030 and 51% by 2045 (1). Thus, the establishment of a promising therapeutic strategy for diabetes is an urgent task. Type 1 diabetes and type 2 diabetes are characterized by insufficient insulin secretion due to reduced numbers and/or function of pancreatic β-cells (2–6); thus, preserving, expanding, and improving β-cell function and/or mass represent fundamental therapeutic approaches to the treatment of diabetes (7).

Glucokinase, which phosphorylates glucose to form glucose-6-phosphate, is expressed in organs with an integrated role in glucose sensing (8). In pancreatic β-cells, glucose phosphorylation with glucokinase is the rate-limiting step in insulin secretion. Glucokinase activation ultimately stimulates insulin secretion, whereas its inactivation leads to its impairment. Mice with glucokinase haploinsufficiency in pancreatic β-cells exhibit mild hyperglycemia associated with impaired insulin secretion (9). In liver, glucose phosphorylation by glucokinase initiates glucose uptake and promotes glycogen synthesis, leading to lowering of the blood glucose level. Because of its central role in glucose homeostasis, glucokinase was targeted for drug development aiming to augment its activity (10,11). Since 2003, numerous glucokinase activators (GKAs) have been developed, and their ability to lower blood glucose levels has been demonstrated in several animal models of type 2 diabetes (10–16). Moreover, we (17,18) and others (19,20) demonstrated that GKAs have can induce β-cell proliferation in addition to augmenting insulin secretion in pancreatic β-cells and glucose uptake in liver.

However, phase 2 clinical trials of some GKAs showed their unsustained effects on glycemic control (21–23). One

[1]Department of Rheumatology, Endocrinology, and Nephrology, Faculty of Medicine and Graduate School of Medicine, Hokkaido University, Sapporo, Japan
[2]Division of Diabetes and Obesity, Faculty of Medicine and Graduate School of Medicine Hokkaido University, Sapporo, Japan
[3]Clinical Research and Medical Innovation Center, Hokkaido University Hospital, Sapporo, Japan
[4]Department of Endocrinology and Metabolism, Graduate School of Medicine, Yokohama City University, Yokohama, Japan

Corresponding author: Akinobu Nakamura, akinbo@tim.hi-ho.ne.jp

Received 27 August 2020 and accepted 22 January 2021

This article contains supplementary material online at https://doi.org/10.2337/figshare.13626674.

of the plausible reasons for their unsustainability could be related to a toxic effect of GKAs on pancreatic β-cells. This hypothesis was elegantly demonstrated using a mouse model of genetic activation of β-cell–specific glucokinase (24). That is, the augmentation of glucose signaling by glucokinase activation led to an initial increase in insulin secretion and β-cell proliferation, but was subsequently associated with β-cell failure (11). This initial augmentation and subsequent β-cell insufficiency were also observed in type 2 diabetes (24).

These observations suggest that optimizing excess glucose signaling in β-cells by reducing glucokinase activity could prevent β-cell failure due to excess glucose influx, leading to improved glucose tolerance in diabetes by preserving β-cell quality and quantity. To test this paradoxical hypothesis, we investigated the effect of glucokinase haploinsufficiency in pancreatic β-cells on glucose tolerance and β-cell function and mass in a mouse model of diabetes.

RESEARCH DESIGN AND METHODS

Animals

$Lepr^{db/+}$ (*db/+*) mice were purchased from Oriental Yeast Co. (Tokyo, Japan). These were crossed with Gck^{tm1Tka}/Gck^{+} ($Gck^{+/-}$) mice (9), generating $Gck^{+/-}$*db/+* mice. These mice were subsequently crossed to generate $Gck^{+/+}$*db/+*, $Gck^{+/-}$*db/+*, $Gck^{+/+}$*db/db*, and $Gck^{+/-}$*db/db* mice. The mutant *Gck* allele in these mice affects the expression of the neuroendocrine isoform of glucokinase but not that of the hepatic isoform (9). Animals were given free access to drinking water and food. The room temperature was maintained at 25°C. Standard chow (MF; Oriental Yeast Co. Ltd.) was provided. Mice were housed two to three animals per cage for all experiments under controlled ambient conditions with a 12-h light/dark cycle (lights on at 7 A.M.) and maintained in accordance with standard animal care procedures based on institutional guidelines. This study was approved by the Animal Use Committee of Hokkaido University Graduate School of Medicine and was conducted in compliance with the Animal Use Guidelines of Hokkaido University.

Measurement of Biochemical Parameters

Blood glucose level was determined using a Glutestmint portable glucose meter (Sanwa Chemical Co., Nagoya, Japan). Insulin levels were measured using an insulin ELISA kit (Morinaga Institute of Biological Science, Yokohama, Japan). Plasma levels of free fatty acids, triglycerides, and ALT were assayed by enzymatic methods (Wako Pure Chemical Industries Ltd., Osaka, Japan).

Oral Glucose Tolerance Test

For the oral glucose tolerance test (OGTT), mice were fasted for 16 hours before being orally loaded with glucose (0.5 mg/g body wt). Blood samples were collected at 0, 15, 30, 60, and 120 min after glucose administration to determine the blood glucose levels.

Insulin Tolerance Test

Insulin tolerance tests were performed under fasting conditions. Human regular insulin (4 units/kg body wt) was injected intraperitoneally, and blood samples were collected before and at 30, 60, 90, and 120 min after the injection.

β-Cell Morphology and Immunohistochemistry

Isolated pancreata were immersion fixed in 4% paraformaldehyde. The tissue was routinely processed for paraffin embedding, and 5-μm sections mounted on glass slides were immunostained with goat anti–rabbit insulin antibody (diluted 1:1,000; Proteintech Group Inc., Rosemont, IL). We analyzed two sections of each pancreas that were 50 μm apart. β-Cell area was calculated using a BZ-II analyzer (Keyence Co., Osaka, Japan). β-Cell mass was estimated for each animal by determining the β-cell area as a proportion of total pancreatic area per animal and multiplying this proportion by the pancreas weight. For immunofluorescence, tissue sections were incubated overnight at 4°C with the primary antibodies listed in Supplementary Table 1. After rinsing with PBS, tissues were incubated with secondary antibodies for 60 min (diluted 1:200) using previously described procedures (25) (Supplementary Table 1). Immunofluorescence images were acquired using a BZ-II analyzer (Keyence Co.) according to the manufacturer's instructions.

Islet Isolation and Glucose-Stimulated Insulin Secretion Assay

Islets were isolated using collagenase from *Clostridium histolyticum* (Sigma-Aldrich, St. Louis, MO) according to the manufacturer's instructions. Krebs-Ringer-HEPES buffer (KRBH) was prepared as described previously (17). Isolated islets were preincubated for 30 min at 37°C in 500 μL KRBH with 2.8 mmol/L glucose. Subsequently, islets were transferred for a 90-min incubation in 500 μL KRBH in low (5.6 mmol/L) or high (22 mmol/L) glucose concentrations. After incubation, medium was collected and stored at −20°C. To determine the insulin content, isolated islets were incubated in acid ethanol, and the insulin concentration in the assay buffer was determined using an insulin ELISA kit (Morinaga Institute of Biological Science).

Real-time Quantitative PCR Analysis

Total RNA was extracted with an RNeasy Mini Kit (Qiagen, Hilden, Germany) and used as the starting material for cDNA preparation. Real-time PCR was performed in duplicate using a 7500 Fast Real Time PCR system with power SYBR Green PCR Master Mix (Applied Biosystems, Foster City, CA). Regarding the islet experiments, data were normalized to GAPDH expression. The primer sequences used are listed in Supplementary Table 2.

Microarray Analysis

Total RNA from isolated islets was extracted with an RNeasy Mini Kit (Qiagen). The mRNA expression profiles

were determined using a Clariom S Mouse Gene 2.0 ST array (Thermo Fisher Scientific Inc., Waltham, MA). Differentially expressed genes were defined as genes that showed at least a 1.5-fold change.

Metabolome Analysis

Approximately 5 mg of frozen isolated islets were plunged into 450 μL of 50% acetonitrile/Milli-Q water containing internal standards (H3304–1002; Human Metabolome Technologies, Inc., Tsuruoka, Japan) at 0°C to inactivate enzymes. The tissue was homogenized twice at 1,500 rpm for 120 s using a tissue homogenizer (Micro Smash MS100R; Tomy Digital Biology Co., Ltd., Tokyo, Japan), and the homogenate was centrifuged at 2,300*g* and 4°C for 5 min. Subsequently, 400 μL of the upper aqueous layer was centrifugally filtered through a 5-kDa cutoff filter (Millipore, Billerica, MA) at 9,100*g* and 4°C for 120 min to remove proteins. The filtrate was centrifugally concentrated and resuspended in 25 μL of Milli-Q water for capillary electrophoresis mass spectrometry analysis. Metabolome measurements were carried out through a facility service at Human Metabolome Technologies, Inc. Hierarchical cluster analysis was performed using the software PeakStat and SampleStat (Human Metabolome Technologies, Inc.). Detected metabolites were plotted on metabolic pathway maps using Visualization and Analysis of Networks containing Experimental Data (VANTED) software (26).

Statistics

Results are expressed as means ± SD. Differences between two groups were assessed using Student *t* test. Individual comparisons between more than two groups were performed using ANOVA followed by a post hoc Bonferroni test. Survival times were assessed by log-rank test. $P < 0.05$ was considered statistically significant.

Data and Resource Availability

The data sets are available from the corresponding author upon reasonable request.

RESULTS

Effect of Glucokinase Haploinsufficiency in *db/db* Mice on Glucose Tolerance and β-Cell Mass

To examine whether glucokinase inhibition affects glucose tolerance in vivo, $Lepr^{db/+}$ (*db/+*) mice were crossed with $Gck^{+/-}$ mice (9), generating $Gck^{+/-}db/+$ mice. Then we crossed and generated $Gck^{+/+}db/+$, $Gck^{+/-}db/+$, $Gck^{+/+}db/db$, and $Gck^{+/-}db/db$ mice, and compared their metabolic phenotypes. $Gck^{+/+}db/db$ and $Gck^{+/-}db/db$ mice gained significantly more body weight than did $Gck^{+/+}db/+$ or $Gck^{+/-}db/+$ mice (Fig. 1*A* and Supplementary Fig. 1*A*). Although $Gck^{+/+}db/+$ and $Gck^{+/-}db/+$ mice had similar weight gain, $Gck^{+/-}db/db$ mice had slightly but significantly greater weight gain compared with $Gck^{+/+}db/db$ mice (Fig. 1*A* and Supplementary Fig. 1*A*). The fed glucose levels of $Gck^{+/-}db/+$ mice were higher than those of $Gck^{+/+}db/+$ mice, as described previously (9,27,28), whereas those of $Gck^{+/-}db/db$ mice conversely decreased after 13 weeks of age and remained significantly lower than those of $Gck^{+/+}db/db$ mice after 20 weeks of age (Fig. 1*B* and Supplementary Fig. 1*B*). There was no difference in food intake between the $Gck^{+/+}db/db$ and $Gck^{+/-}db/db$ mice (Supplementary Fig. 2*A*).

Furthermore, the OGTT results when the mice were 23 weeks old indicated that $Gck^{+/-}db/db$ mice were significantly more glucose tolerant than were the $Gck^{+/+}db/db$ mice (Fig. 1*C* and *D*). There were no difference in insulin sensitivity measured by the insulin tolerance test, lipid profile, or hepatic function between the $Gck^{+/+}db/db$ and $Gck^{+/-}db/db$ mice (Supplementary Fig. 2*B*–*E*). $Gck^{+/-}db/db$ mice had significantly higher plasma insulin levels than did the $Gck^{+/+}db/db$ mice (Fig. 1*E*). Ex vivo glucose-stimulated insulin secretion of isolated islets from $Gck^{+/-}db/db$ mice significantly increased compared with that of $Gck^{+/+}db/db$ mice (Fig. 1*F*). Interestingly, the survival time of $Gck^{+/-}db/db$ mice was significantly longer than that of $Gck^{+/+}db/db$ mice (Fig. 1*G*).

Subsequently, we evaluated pancreatic β-cell mass of these mice when they were 24 weeks old. Histological analysis showed that β-cell area in $Gck^{+/-}db/db$ mice was significantly greater than that in $Gck^{+/+}db/db$ mice, although $Gck^{+/+}db/+$ and $Gck^{+/-}db/+$ mice had similar β-cell area (Fig. 2*A* and *B*). There were no differences in pancreatic weight between the $Gck^{+/+}db/+$ and $Gck^{+/-}db/+$ mice and between the $Gck^{+/+}db/db$ and $Gck^{+/-}db/db$ mice (Fig. 2*C*). As a result, β-cell mass in $Gck^{+/-}db/db$ mice significantly increased compared with that of the other three groups (Fig. 2*D*). On the other hand, there was no difference in the ratio of the number of α-cells to the total combined number of α- and β-cells in the pancreatic islets of the $Gck^{+/+}db/db$ and $Gck^{+/-}db/db$ mice (Supplementary Fig. 3). Taken together, these results show glucose tolerance in $Gck^{+/-}db/db$ mice was ameliorated by augmentation of insulin secretion associated with increasing β-cell mass, compared with $Gck^{+/+}db/db$ mice.

Effect of Glucokinase Haploinsufficiency in *db/db* Mice on Exhaustive Changes in Gene Expression

To explore a striking difference in gene expression of islets from $Gck^{+/+}db/db$ and $Gck^{+/-}db/db$ mice, DNA microarray analysis was performed using islets isolated from these mice when they were 10 weeks old. Of note, when aged 10 weeks, fed blood glucose levels and glucose tolerance evaluated by OGTT in $Gck^{+/-}db/db$ mice were equivalent to those in $Gck^{+/+}db/db$ mice (Fig. 1*B* and Supplementary Fig. 4*A*). β-Cell mass was also comparable between the two groups of mice (Supplementary Fig. 4*B*). Microarray analysis revealed 1,484 genes were differentially expressed 1.5 fold, with statistical significance in islets isolated from $Gck^{+/-}db/db$ versus $Gck^{+/+}db/db$ mice. Among these, 432 were upregulated and 1,052 were downregulated. Pathway analyses showed significant changes in seven upregulated and 22 downregulated pathways (Table 1). In particular,

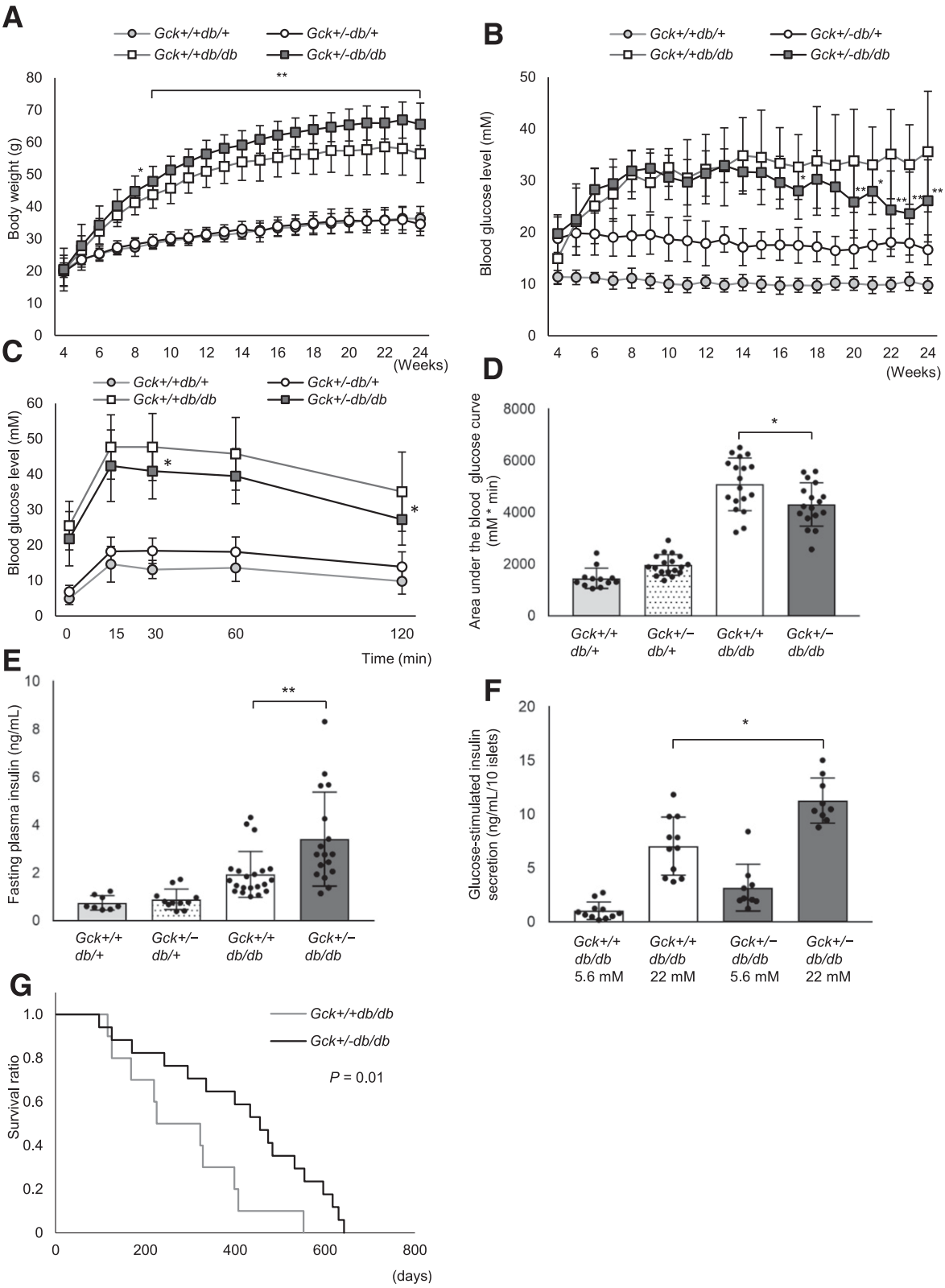

Figure 1—Effects of glucokinase haploinsufficiency on metabolic changes and glucose tolerance. *A* and *B*: Changes in (*A*) body weight and (*B*) blood glucose levels in the $Gck^{+/+}db/+$, $Gck^{+/-}db/+$, $Gck^{+/+}db/db$, and $Gck^{+/-}db/db$ mice ($n = 15$–18) (*$P < 0.05$; **$P < 0.01$ vs. $Gck^{+/+}db/db$). *C*: Blood glucose levels during the OGTT in the $Gck^{+/+}db/+$, $Gck^{+/-}db/+$, $Gck^{+/+}db/db$, and $Gck^{+/-}db/db$ mice after a 16-h fast at 23 weeks of age ($n =$ 12–18). *D*: Area under the curve of glucose excursion during the OGTT in the $Gck^{+/+}db/+$, $Gck^{+/-}db/+$, $Gck^{+/+}db/db$, and $Gck^{+/-}db/db$ mice after a 16-h fast at 23 weeks of age ($n = 12$–18) (*$P < 0.05$ vs. $Gck^{+/+}db/db$). *E*: Fasting plasma insulin level in the $Gck^{+/+}db/+$, $Gck^{+/-}db/+$, $Gck^{+/+}db/db$, and $Gck^{+/-}db/db$ mice after a 16-h fast at 23 weeks of age ($n = 8$–21). *F*: Glucose-stimulated insulin secretion in isolated islets from the $Gck^{+/+}db/db$ and $Gck^{+/-}db/db$ mice at 23 weeks of age ($n = 9$–11). *G*: The survival time of the $Gck^{+/+}db/db$ and $Gck^{+/-}db/db$ mice ($n = 10$–17). Values are means ± SD. *P* values were determined using ANOVA followed by post hoc Bonferroni test in *A*–*F*. Survival times were assessed by log-rank test in *G*. *$P < 0.05$; **$P < 0.01$.

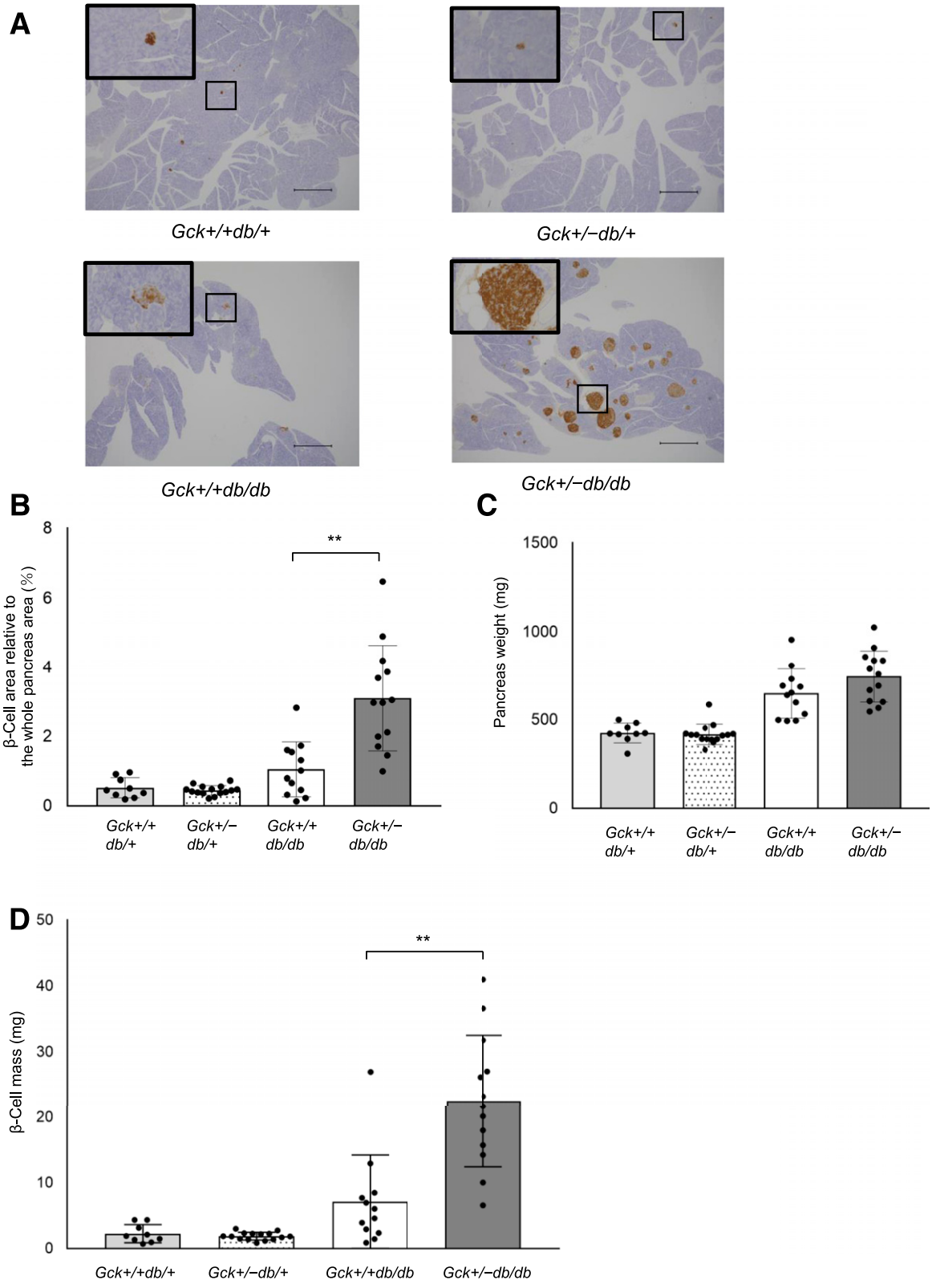

Figure 2—Effect of glucokinase haploinsufficiency on β-cell morphology in mice aged 24 weeks. *A*: Immunohistological analysis of pancreatic islets from the four groups; *Gck*$^{+/+}$*db/+*, *Gck*$^{+/-}$*db/+*, *Gck*$^{+/+}$*db/db*, and *Gck*$^{+/-}$*db/db* mice. β-Cells are stained brown. Black scale bars represent 500 μm. *B–D*: Quantitation of (*B*) β-cell area, (*C*) pancreatic weight, and (*D*) β-cell mass in the *Gck*$^{+/+}$*db/+*, *Gck*$^{+/-}$*db/+*, *Gck*$^{+/+}$*db/db*, and *Gck*$^{+/-}$*db/db* mice (n = 9–15). Values are means ± SD. *P* values were determined using ANOVA followed by post hoc Bonferroni test. $^{**}P < 0.01$.

upregulated pathways included the Ptf1a-related regulatory pathway, such as NK6 homeobox 1 (*Nkx6.1*) and pancreatic and duodenal homeobox 1 (*Pdx1*), which play important roles in β-cell function and maturation, whereas the downregulated pathways included metabolic stress and β-cell damage-related pathways, such as the oxidative stress and inflammatory response pathway.

Regarding glucose metabolism, we found the expression of some genes that encode glycolytic enzymes, including aldolase B (*Aldob*), enolase 1 (*Eno1*), and glucose phosphate isomerase 1 (*Gpi1*), was lower in $Gck^{+/-}db/db$ mice than in $Gck^{+/+}db/db$ mice (Supplementary Table 4). In contrast, the expression of genes that encode enzymes involved in the tricarboxylic acid (TCA) cycle, including pyruvate carboxylase (*Pcx*), isocitrate dehydrogenase 3, γ (*Idh3g*), isocitrate dehydrogenase 2 (*Idh2*), and aconitase 2 (*Aco2*), was significantly higher or tended to be higher in $Gck^{+/-}db/db$ mice. Moreover, the expression of the gene encoding pyruvate dehydrogenase kinase, isoenzyme 1 (*Pdk1*), which limits the entry of pyruvate into the TCA cycle, was significantly lower in $Gck^{+/-}db/db$ mice than in $Gck^{+/+}db/db$ mice (Table 1 and Supplementary Tables 3 and 4). These results suggest glucokinase haploinsufficiency is associated with greater expression of β-cell–associated transcription factors, less expression of metabolic stress-related factors, and altered expression of glucose metabolism–related factors in *db/db* mice.

Effect of Glucokinase Haploinsufficiency in *db/db* Mice on β-Cell Proliferation and Death, and β-Cell–Associated Transcription Factors

Although there was no difference in β-cell mass between the $Gck^{+/+}db/db$ and $Gck^{+/-}db/db$ mice aged 10 weeks (Supplementary Fig. 4*B*), insulin content in isolated islets of $Gck^{+/-}db/db$ mice was significantly higher than in $Gck^{+/+}db/db$ mice (Fig. 3*A*). Moreover, the β-cell proliferation rate evaluated by Ki67 staining was significantly greater in $Gck^{+/-}db/db$ mice (Fig. 3*B*). There were no differences in the β-cell apoptotic rate, evaluated using fluorometric TUNEL staining, or in the expression of islet progenitor cell markers, including neurogenin 3 (*Neurog3*) and aldehyde dehydrogenase 1a3 (*Aldh1a3*), between the two groups of mice at 10 weeks of age (Supplementary Fig. 5). However, the rate of TUNEL-positive β-cells in $Gck^{+/-}db/db$ mice tended to be lower than in $Gck^{+/+}db/db$ mice at 24 weeks of age (Supplementary Fig. 6).

In addition, to assess fibrosis in these pancreata, Azan staining was performed. This showed fibrosis in and around the islets of $Gck^{+/+}db/db$, but this was less marked in $Gck^{+/-}db/db$ mice (Supplementary Fig. 7). This greater proliferation and lesser cell damage could explain the greater β-cell mass in $Gck^{+/-}db/db$ mice at 24 weeks of age (Fig. 2*D*). In addition, quantitative real-time PCR indicated that cell proliferation and cell cycle–related gene expression levels of *Ki67*, cyclin B1 (*Ccnb1*), and cyclin D2 (*Ccnd2*) in $Gck^{+/-}db/db$ mice, but not cyclin D1 (*Ccnd1*) nor cyclin D3 (*Ccnd3*), were significantly increased compared with those in $Gck^{+/+}db/db$ mice (Fig. 3*C*).

In agreement with the findings of the microarray analysis, mRNA expression levels of β-cell–associated transcription factors, including v-maf musculoaponeurotic fibrosarcoma oncogene family, protein A (*Mafa*), *Nkx6.1*, and *Pdx1*, were significantly increased in $Gck^{+/-}db/db$ mice (Fig. 3*D*). Immunohistochemical analysis revealed an increase in the rate of MafA- and Nkx6.1-positive β-cells in $Gck^{+/-}db/db$ mice in comparison with $Gck^{+/+}db/db$ mice (Fig. 3*E–H*), whereas there was no difference in the rate of positive β-cells between the $Gck^{+/+}db/+$ and $Gck^{+/-}db/+$ mice, and the rate in the $Gck^{+/+}db/db$ mice was lower than those in the $Gck^{+/+}db/+$ and $Gck^{+/-}db/+$ mice (Supplementary Fig. 8). Furthermore, the MafA and Nkx6.1 protein expression levels were higher in $Gck^{+/-}db/db$ mice (Supplementary Fig. 9). These findings suggest that $Gck^{+/-}db/db$ mice displayed enhanced insulin content and β-cell proliferation by increasing expression levels of transcription factors associated with β-cell function, compared with $Gck^{+/+}db/db$ mice.

Effect of Glucokinase Haploinsufficiency in *db/db* Mice on Stress Markers and Glucose Metabolism

Because oxidative stress inactivates the β-cell function–associated transcription factors (29), we considered whether increasing expression levels of these transcription factors could be due to reduced metabolic stress in $Gck^{+/-}db/db$ mice. The microarray analysis revealed that the expression levels of metabolic stress-related genes were downregulated in $Gck^{+/-}db/db$ mice compared with $Gck^{+/+}db/db$ mice (Table 1 and Supplementary Table 3). Similarly, in addition to activating transcription factor 3 (*Atf3*), mRNA levels of cytochrome b-245 α polypeptide (*Cyba*) and neutrophil cytosolic factor 1 (*Ncf1*), which are parts of the NAD phosphate oxidase complex, were significantly decreased in $Gck^{+/-}db/db$ mice by quantitative real-time PCR (Fig. 4*A*). Subsequently, we examined mitochondrial morphology, which was commonly affected by metabolic stress, in β-cells of the two mouse groups. As shown in Fig. 4*B*, Tom20 staining of β-cells from $Gck^{+/+}db/db$ mice was heterogeneous, representing fragmentation of the mitochondrial network (30). By contrast, its staining of β-cells from $Gck^{+/-}db/db$ mice was less heterogeneous and extended throughout β-cells. Quantitatively, the mitochondrial area in β-cells of $Gck^{+/-}db/db$ mice was significantly larger than that of $Gck^{+/+}db/db$ mice (Fig. 4*C*).

Next, we compared glucose metabolism–associated mRNA expression levels, including glycolysis and the TCA cycle in islets between the two mouse groups, because significant changes in their expression levels were observed by microarray analysis (Table 1 and Supplementary Table 3). Not only *Pcx* upregulation and *Aldob* downregulation (not significantly) but also 6-phosphofructo-2-kinase/fructose-2,6- biphosphatase 3 (*Pfkfb3*) downregulation were observed in $Gck^{+/-}db/db$ mice compared with $Gck^{+/+}db/db$

Table 1—Pathway analysis from the microarray data

Pathway Name	No. of Changed Genes	Total Genes	*Z* score	*P* value	Gene symbol
Ratio > 1.5					
Mm_Amino_Acid_metabolism_WP662_71177	8	95	4.56	7.14E−04	*Hnmt Hadh Hibadh Ddc Pycr1 Auh Mut Pcx*
Mm_GPCRs_Class_B_Secretin-like_WP456_69131	3	22	3.96	0.012	*Adgrl3 Gipr Glp1r*
Mm_Ptf1a_related_regulatory_pathway_WP201_69113	2	11	3.89	0.025	*Pdx1 Nkx6–1*
Mm_G1_to_S_cell_cycle_control_WP413_84705	4	61	2.60	0.035	*E2f1 Ccnd2 Cdc45 Cdkn1a*
Mm_G_Protein_Signaling_Pathways_WP232_89955	5	91	2.44	0.036	*Pde7a Pde4b Gng12 Akap13 Akap5*
Mm_Non-odorant_GPCRs_WP1396_69993	10	266	2.13	0.041	*Adgrb3 P2ry1 Gabbr2 Adgrl3 Gipr Ackr2 Sstr3 Glp1r Mc5r Adra2a*
Mm_Metapathway_biotransformation_WP1251_69747	6	133	2.13	0.049	*Hnmt Akr1b10 Chst11 Gal3st1 Gpx2 Hs3st6*
Ratio < 0.67					
Mm_Cytoplasmic_Ribosomal_Proteins_WP163_78425	34	79	10.40	1.38E−11	*Rpl37a Rpl7 Rpl7a Rpl35 Rps3a1 Rpl34 Rps20 Rps8 Rpl9 Rpl37rt Rps5 Rps19 Rps16 Rpl27a Rplp2 Rps11 Rps13 Rps15a Rpl13 Rps25 Rpl36a Rpl39 Rps4× Rps12 Rpl26 Rps27a Rpl23a Rps7 Rpl37 Rpl3 Rpl35a Rps28 Rps14 Fau*
Mm_Focal_Adhesion_WP85_82887	40	184	5.88	3.22E−06	*Col3a1 Lamb3 Col5a2 Fn1 Lamc1 Col5a1 Lamc3 Pdgfc Jun Hgf Pdgfra Spp1 Pxn Actb Col1a2 Cav2 Cav1 Met Vwf Itgam Dock1 Col4a2 Pdgfd Lamb2 Figf Flna Lama4 Igf1 Lama2 Col6a2 Vtn Col1a1 Erbb2 Itgb4 Rhob Itgb8 Shc3 Mylk Lama3 Pdgfrb*
Mm_PodNet-_protein-protein_interactions_in_the_podocyte_WP2310_82879	56	315	5.26	9.80E−06	*Sulf1 Cfh Lamc1 Tgfb2 Olfm1 Angptl2 Notch2 Cyr61 Hspg2 Pdpn Agrn Spp1 Pxn Slc29a4 Arpc1b Actb Smurf1 Met Cxcl12 Plaur Tgfb1 Cd151 Bcam Fcgrt Nr2f2 Sh2d4a Nrp1 Palld Myo1e Lamb2 Tagln Smad3 Tgfbr2 Ctgf Igf1 Tcf21 Col18a1 Myh10 Itgb4 Wwc1 Cxcl16 Egln3 Tgfb3 Nid1 Dbn1 Ctsl Scel Bmp4 Lgals1 Angpt1 Igsf5 Crim1 Epas1 Ezr Notch3 Plce1*
Mm_XPodNet_-_protein-protein_interactions_in_the_podocyte_expanded_by_STRING_WP2309_82878	113	825	4.44	2.24E−05	*Sulf1 Nrp2 Fn1 Cfh Lamc1 Tgfb2 Vim Olfm1 Lamc3 Angptl2 Enkur Zeb2 Eng Notch2 Ngf Csf1 Cyr61 Lyn Nr4a3 Hspg2 Pdpn Agrn Cdk6 Ptpn13 Spp1 Pxn Slc29a4 Arpc1b Eln Cldn4 Actb Smurf1 Cav1 Met Fbln2 Bhlhe40 Cxcl12 Vwf Plaur Tgfb1 Gab2 Arrb1 Htra1 Cd151 Cdc42ep5 Bcam Zfp36 Fcgrt Nr2f2 Nrip3 Sh2d4a Cdh5 Sntb2 Plcg2 Nrp1 Palld Gab1 Anxa2 Myo1e Lamb2 Tagln Smad3 Rab8b Tgfbr2 Trf L1cam Ctgf Gja1 Igf1 Cdk17 Tcf21 Lama2 Hk1 Col18a1 Syt1 Gnb2l1 Myh10 Tax1bp3 Vtn Itgb4 Wwc1 Cxcl16 Abcc3 Pecam1 Dock4 Egln3 Tgfb3 Nid1 Actn2 Dbn1 Ctsl Scel Bmp4 Ajuba Sorbs3 Cdc42ep1 Lgals1 Angpt1 Plec Cldn8 Igsf5 Ltbp1 Crim1 Epas1 Ezr Notch3 Pdgfrb Csf1r Rin1 Ffar4 Plce1 Sorbs1 Blnk*
Mm_Prostaglandin_Synthesis_and_Regulation_WP374_69204	11	31	5.07	5.14E−04	*Hsd11b1 Ptgs1 S100a6 S100a10 Ptger3 Anxa3 Tbxas1 Hpgd Anxa2 Ednrb Anxa1*
Mm_Endochondral_Ossification_WP1270_87973	16	62	4.53	6.24E−04	*Ddr2 Tgfb2 Fgfr3 Spp1 Mgp Tgfb1 Serpinh1 Sox6 Fgfr1 Timp3 Igf1 Enpp1 Sox9 Mef2c Ctsl Slc38a2*
Mm_Complement_Activation_Classical_Pathway_WP200_72061	7	16	4.78	2.13E−03	*C1qb C1qc C1ra C1s1 C7 Masp1 C4b*
Mm_Spinal_Cord_Injury_WP2432_87679	19	96	3.59	3.52E−03	*Selp Fcgr2b Vim Rhoc Tlr4 Tgfb1 Rgma Zfp36 Pirb Mmp12 Icam1 Gja1 Sox9 Rhob Rtn4r Egr1 Aqp4 Sema6a Anxa1*

Continued on p. 924

Table 1—Continued

Pathway Name	No. of Changed Genes	Total Genes	*Z* score	*P* value	Gene symbol
Mm_Complement_and_Coagulation_Cascades_WP449_71733	14	61	3.72	4.73E−03	*Cfh Tfpi Serping1 C1qb C1qc C1ra Vwf C1s1 Plaur C7 Pros1 Masp1 C4b Cfb*
Mm_Macrophage_markers_WP2271_69962	5	10	4.47	6.10E−03	*Cd52 Cd163 Lyz2 Cd68 Cd14*
Mm_TYROBP_Causal_Network_WP3625_90841	13	58	3.48	7.46E−03	*Dpyd C1qc Spp1 Tyrobp Kcne3 Itgam Igsf6 Elf4 Cxcl16 Npc2 Lhfpl2 Slc7a7 Zfp36l2*
Mm_Focal_Adhesion-PI3K-Akt-mTOR-signaling_pathway_WP2841_89989	44	318	2.86	0.011	*Col3a1 Lamb3 Col5a2 Fn1 Lamc1 Col5a1 Lamc3 Pfkfb3 Pdgfc Ngf Csf1 Slc2a1 Hgf Fgfr3 Pdgfra Spp1 Ppargc1a Col1a2 Met Vwf Itgam Fgfr2 Col4a2 Fgfr1 Pdgfd Lamb2 Figf Lama4 Igf1 Kitl Lama2 Col6a2 Vtn Col1a1 Itgb4 Itgb8 Fgfr4 Osmr Angpt1 Epas1 Lama3 Pdgfrb Csf1r Ppp2r2b*
Mm_Oxidative_Stress_WP412_89965	7	27	3.01	0.021	*Cat Mgst1 Hmox1 Mt1 Nfix Junb Cyba*
Mm_Alpha6-Beta4_Integrin_Signaling_Pathway_WP488_72049	13	66	2.95	0.021	*Lamb3 Lamc1 Vim Met Cd151 Lamb2 Smad3 Ar Lama2 Erbb2 Itgb4 Plec Lama3*
Mm_Striated_Muscle_Contraction_WP216_87693	10	45	3.02	0.023	*Des Vim Myl9 Tpm3 Tpm2 Tpm4 Tpm1 Dmd Actn2 Acta2*
Mm_Primary_Focal_Segmental_Glomerulosclerosis_FSGS_WP2573_89874	13	70	2.71	0.026	*Vim Jag1 Tlr4 Agrn Plaur Tgfb1 Cd151 Myo1e Lamb2 Vtn Itgb4 Ctsl Plce1*
Mm_Matrix_Metalloproteinases_WP441_69114	7	29	2.79	0.028	*Mmp23 Mmp2 Mmp15 Mmp12 Timp3 Timp2 Mmp14*
Mm_Inflammatory_Response_Pathway_WP458_78438	7	30	2.68	0.032	*Col3a1 Fn1 Lamc1 Col1a2 Lamb2 Vtn Col1a1*
Mm_Microglia_Pathogen_Phagocytosis_Pathway_WP3626_87399	9	41	2.83	0.034	*Vav3 Lyn C1qb C1qc Arpc1b Tyrobp Itgam Plcg2 Cyba*
Mm_Factors_and_pathways_affecting_insulin-like_growth_factor_(IGF1)-Akt_signaling_WP3675_90178	7	31	2.58	0.037	*Igfbp5 Pdk1 Pld1 Ppargc1a Smad3 Igf1 Igfbp4*
Mm_Irinotecan_Pathway_WP475_69144	3	7	3.08	0.045	*Bche Abcg2 Ces1d*
Mm_Statin_Pathway_WP1_73346	5	19	2.58	0.046	*Pltp Abca1 Scarb1 Apoe Lrp1*

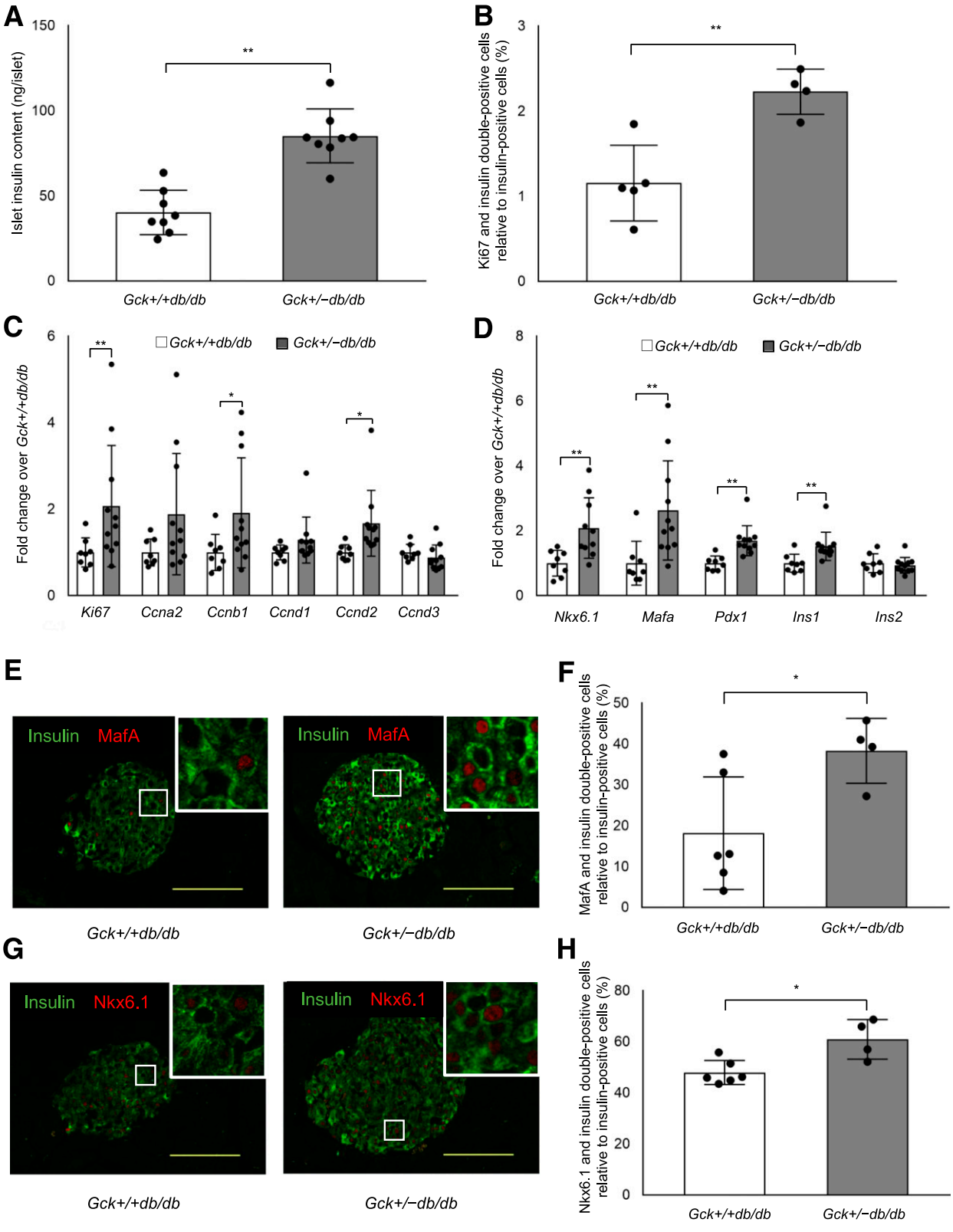

Figure 3—Effect of glucokinase haploinsufficiency on β-cell proliferation and transcription factors in *db/db* mice aged 10 weeks. *A*: Islet insulin content in the $Gck^{+/+}$*db/db* and $Gck^{+/-}$*db/db* mice ($n = 8$). *B*: Proliferation rate of β-cells assessed by Ki67 staining in the $Gck^{+/+}$*db/db* and $Gck^{+/-}$*db/db* mice ($n = 4$–5). *C*: Gene expression levels of *Ki67*, *Ccna2*, *Ccnb1*, *Ccnd1*, *Ccnd2*, and *Ccnd3* in the $Gck^{+/+}$*db/db* and $Gck^{+/-}$*db/db* mice by real-time quantitative PCR ($n = 8$–11). *D*: Gene expression levels of *Nkx6.1*, *Mafa*, *Pdx1*, *Ins1*, and *Ins2* in the $Gck^{+/+}$*db/db* and $Gck^{+/-}$*db/db* mice by real-time quantitative PCR ($n = 8$–11). *E*: Representative insulin (green) and MafA (red) immunofluorescent staining of pancreas sections from the $Gck^{+/+}$*db/db* and $Gck^{+/-}$*db/db* mice. Yellow scale bars represent 100 μm. *F*: Quantitation of MafA and insulin double-positive cells relative to insulin-positive cells (%) in the $Gck^{+/+}$*db/db* and $Gck^{+/-}$*db/db* mice ($n = 4$–6). *G*: Representative

mice (Fig. 4*D*). These results suggest glucokinase haploinsufficiency could ameliorate metabolic stress, leading to mitochondrial damage reduction, and that it could modify the pattern of gene expressions associated with glucose metabolism in *db/db* mice.

Effect of Glucokinase Haploinsufficiency in *db/db* Mice on Metabolites

The results we report here suggest some differences in intracellular metabolism in islets between the $Gck^{+/+}db/db$ and $Gck^{+/-}db/db$ mice. Therefore, we examined intracellular metabolites in islets of the two mouse groups using metabolomics analysis. Figure 5*A* is a hierarchical cluster analysis heat map of the detected 95 metabolites. This result indicated that alteration in metabolites occurred between the two groups. In detail, glycolytic intermediates and metabolites, including fructose 6-phosphate, pyruvic acid, and lactic acid, were decreased in $Gck^{+/-}db/db$ mice (Fig. 5*B*). In the TCA cycle, isocitric acid was increased in $Gck^{+/-}db/db$ mice when compared with those in $Gck^{+/+}db/db$ mice (Fig. 5*B*). Of note, a step up of the ratio of metabolites ($Gck^{+/-}db/db$ mice to $Gck^{+/+}db/db$ mice) from pyruvic acid or malic acid to citric acid (0.6 → 1.0 and 0.3 → 1.0, respectively) was observed. On the basis of the findings that the expression of genes encoding enzymes involved in the TCA cycle, including *Pcx*, was higher in $Gck^{+/-}db/db$ mice (Fig. 4*D* and Supplementary Table 4) and that the ATP level in $Gck^{+/-}db/db$ mice was double that of $Gck^{+/+}db/db$ mice (Fig. 5*B*), we suggest that the metabolism of the $Gck^{+/-}db/db$ mice is not dominated by glycolysis, as in diabetic islets (31), but is instead shifted toward the TCA cycle and oxidative phosphorylation.

DISCUSSION

In this study, we demonstrated that glucokinase haploinsufficiency in pancreatic β-cells ameliorated glucose tolerance by insulin secretion augmentation associated with the increase in β-cell mass in *db/db* mice. Recently, it was reported that reducing glucokinase activity restored pulsatility and improved pulsatility correlated with enhanced insulin secretion in islets of *db/db* mice (32,33). These results are in agreement with our findings. The strength of our study is our findings about the impact of glucokinase haploinsufficiency on β-cell mass. In addition, we have shown the beneficial effect of glucokinase inactivation on the glucose tolerance of an in vivo model of diabetes.

A mouse model of β-cell–specific genetic activation of glucokinase initially showed greater insulin secretion and β-cell proliferation, but a subsequent progression of β-cell damage (24) and a similar phenotypic progression occurs in *db/db* mice (34). The β-cell mass of the $Gck^{+/+}db/db$ mice was increased at 10 weeks. However, no additional increase was observed at 24 weeks of age (Supplementary Fig. 10). Instead, β-cell damage was more evident in the form of greater fibrosis (Supplementary Fig. 7). These results imply that *Gck* transgenic mice and *db/db* mice have similar β-cell phenotypes, despite differences in obesity and hyperleptinemia. In the islets of *db/db* mice, there is evidence of higher expression of metabolic stress-related genes, lower expression of pancreatic β-cell–associated transcription factors, and mitochondrial damage (35,36). In contrast, we have shown that glucokinase haploinsufficiency in the islets of *db/db* mice reduces the expression of stress genes, increases the expression of the transcription factors, reduces mitochondrial damage, and improves the metabolic pattern. These effects of glucokinase haploinsufficiency could result in greater insulin synthesis and the preservation of β-cell mass under diabetic conditions.

We suggest that glucokinase haploinsufficiency could suppress metabolic stress by reducing the influx of excess glucose metabolites. Our data in the microarray analysis support this notion. Oxidative stress reduction by genetically induced antioxidant-enzyme overexpression or antioxidant therapy improved β-cell function and mass in *db/db* mice (37,38). In this condition, β-cell–associated transcription factors are important for the enhancement of β-cell function and mass. Guo et al. (29) reported that hyperglycemia and oxidative stress lead to β-cell dysfunction by targeting MafA and Nkx6.1 in *db/db* mice and that glutathione peroxidase-1 antioxidant enzyme overexpression in β-cells in *db/db* mice restored MafA, Nkx6.1, and β-cell function. These findings were consistent with our results, indicating that the numbers of MafA- and Nkx6.1-positive β-cells in $Gck^{+/-}db/db$ mice were significantly higher than those in $Gck^{+/+}db/db$ mice. The MafA-producing *db/db* mice had improved glycemic control and augmentation of β-cell function and mass (39), and Nkx6.1 overexpression led to improved glucose-stimulated insulin secretion and enhanced β-cell proliferation (40). Moreover, Taylor et al. (41) demonstrated that Nkx6.1 directly regulates the transcription of genes involved in glucose metabolism, including of Pcx, which plays an important role in metabolizing pyruvate into the TCA cycle. Because the islets of $Gck^{+/-}db/db$ mice had a higher *Pcx* expression level than those of $Gck^{+/+}db/db$ mice, and because the metabolic pattern shifted toward the TCA cycle and oxidative phosphorylation dominance in $Gck^{+/-}db/db$ mice, there is a possibility that the Nkx6.1-induced Pcx increase is involved in the augmentation of β-cell mass (42,43).

insulin (green) and Nkx6.1 (red) immunofluorescent staining of pancreas sections from the $Gck^{+/+}db/db$ and $Gck^{+/-}db/db$ mice. Yellow scale bars represent 100 μm. *H*: Quantitation of Nkx6.1 and insulin double-positive cells relative to insulin-positive cells (%) in the $Gck^{+/+}db/db$ and $Gck^{+/-}db/db$ mice (n = 4–6). Values are means ± SD. P values were determined using Student t test. *$P < 0.05$; **$P < 0.01$.

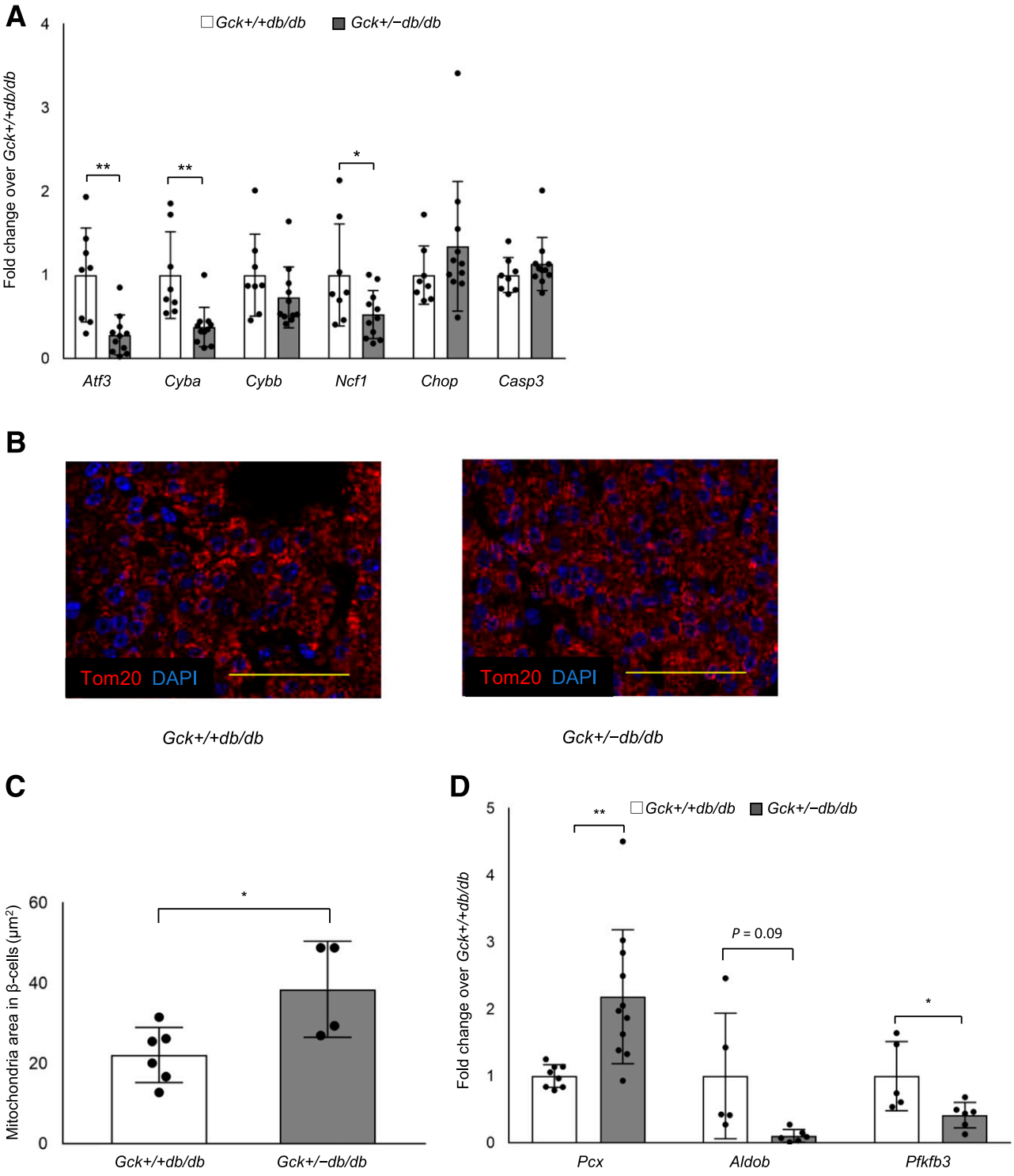

Figure 4—Effect of glucokinase haploinsufficiency on stress markers, mitochondrial network, and metabolic factors in *db/db* mice aged 10 weeks. *A*: Gene expression levels of β-cell–associated oxidative stress. Expression of *Atf3*, *Cyba*, *Cybb*, *Ncf1*, *Chop*, and *Casp3* in the $Gck^{+/+}db/db$ and $Gck^{+/-}db/db$ mice was determined by real-time quantitative PCR (n = 8–11). *B*: Representative Tom20- (red) and DAPI-stained nucleus (blue) immunofluorescent staining of pancreas sections from the $Gck^{+/+}db/db$ and $Gck^{+/-}db/db$ mice. Yellow scale bars represent 50 μm. *C*: Quantitation of the Tom20-positive area inside the insulin-positive area per islet divided by the number of β-cells in the $Gck^{+/+}db/db$ and $Gck^{+/-}db/db$ mice (n = 4–6). *D*: Gene expression levels of *Pcx, Aldob*, and *Pfkfb3* in the $Gck^{+/+}db/db$ and $Gck^{+/-}db/db$ mice determined by real-time quantitative PCR (n = 5–11). Values are means ± SD. *P* values were determined using Student *t* test. $^{*}P < 0.05$; $^{**}P < 0.01$.

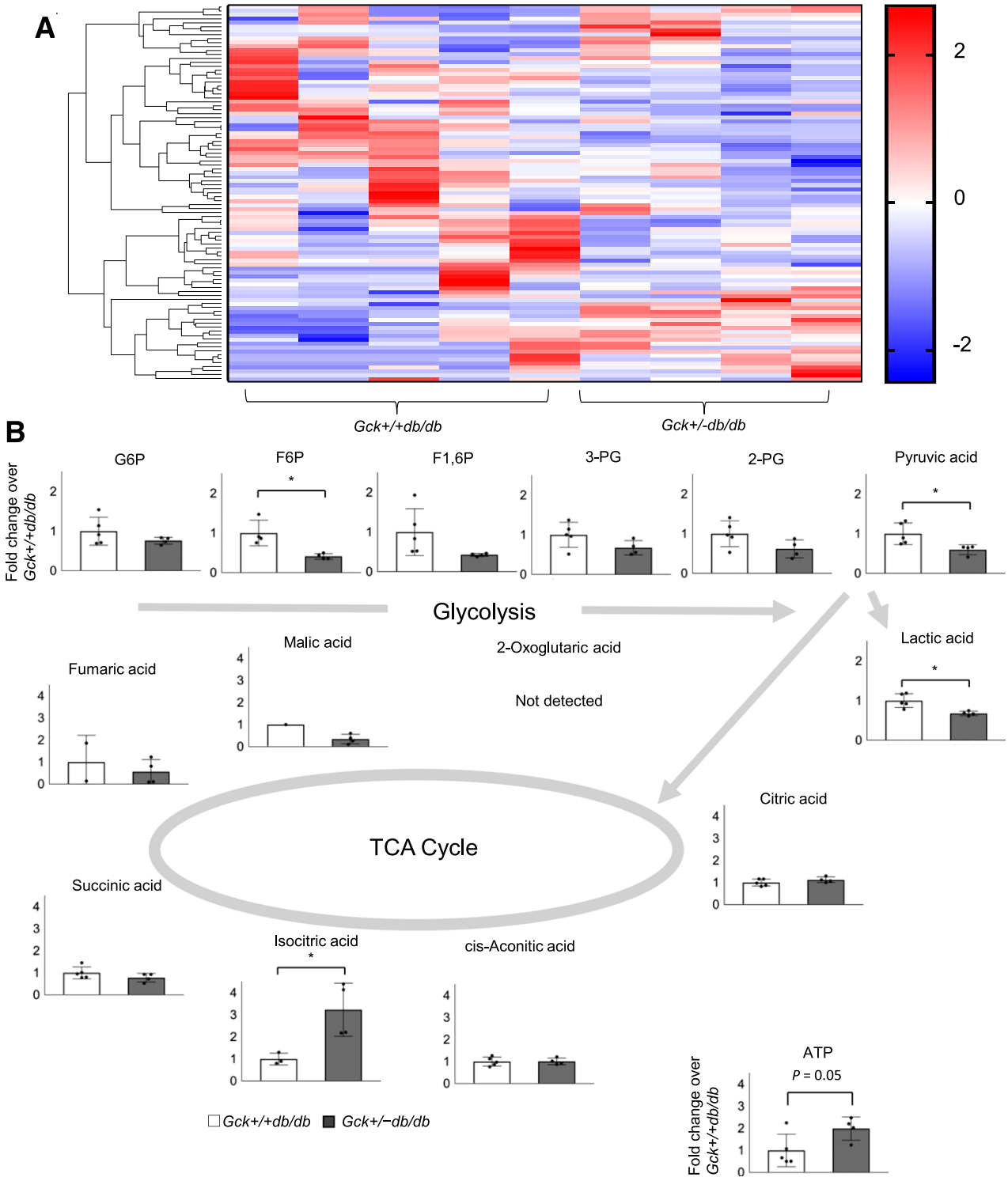

Figure 5— Metabolome analysis in islets of the *Gck*$^{+/+}$*db/db* and *Gck*$^{+/-}$*db/db* mice aged 10 weeks. *A*: Total data for visualization of differentially expressed genes using hierarchical clustering in islets of the *Gck*$^{+/+}$*db/db* and *Gck*$^{+/-}$*db/db* mice ($n = 4$–5). *B*: Main metabolites in glycolysis and the tricarboxylic cycle and ATP contents in islets of the *Gck*$^{+/+}$*db/db* and *Gck*$^{+/-}$*db/db* mice ($n = 4$–5). Values are means ± SD. *P* values were determined using Student *t* test. *$P < 0.05$. G6P, glucose 6-phosphate; F6P, fructose 6-phosphate; F1,6P, fructose 1,6-diphosphate; 3-PG, 3-phosphoglyceric acid; 2-PG, 2-phosphoglyceric acid.

Another possible mechanism is that metabolic stress reduction limits mitochondrial damage. Our data demonstrated an improvement of mitochondrial morphology and a significant decrease of *Pfkfb3* expression in *Gck*$^{+/-}$*db/db* mice. Recently, it was reported that mitochondrial fragmentation followed by increased *Pfkfb3* expression in

β-cells enhanced the aerobic glycolysis that diverted pyruvate acid into lactic acid (30). That is, *Pfkfb3* accelerates the metabolic pattern shift from the TCA cycle and oxidative phosphorylation dominance toward glycolytic pathway dominance, which is known and described as metabolic remodeling. Therefore, decreased *Pfkfb3* expression could affect amelioration of the metabolic remodeling in $Gck^{+/-}$*db/db* mice. Moreover, we need to consider the possibility that a reduction in glucokinase protects pancreatic β-cells from marked increases in intracellular Ca^{2+} in *db/db* mice. It has been reported that large increases in intracellular Ca^{2+} can induce mitochondrial damage and β-cell failure (44). Our gene expression analysis of Ca^{2+} binding and signaling revealed that the expression of the genes encoding S100 calcium-binding protein A6 (*S100a6*) and myocyte enhancer factor 2C (*Mef2c*) in $Gck^{+/-}$*db/db* mice was significantly lower than in $Gck^{+/+}$*db/db* mice, and that the expression of *S100a13* and *S100a4* in $Gck^{+/-}$*db/db* mice tended to be lower than in $Gck^{+/+}$*db/db* mice (Supplementary Table 5). Because S100a6 and S100a4 may represent markers of β-cell excitotoxicity (45), these results suggest glucokinase haploinsufficiency protects pancreatic β-cells against marked increases in intracellular Ca^{2+}, thereby preventing mitochondrial damage and β-cell failure in *db/db* mice.

From a clinical point of view, glycemic control in patients with type 2 diabetes could be achieved either by promoting endogenous insulin secretion or by reducing both hyperglycemia and insulin secretory demand, which leads to providing β-cell rest (46). The latter strategies seem the most promising because they are expected to preserve β-cell mass. Indeed, β-cell proliferation is induced by genetically reducing insulin production in mouse islets and in a human induced pluripotent β-cell–like stem cell model (47,48). Additionally, in a genetic mouse model, less insulin secretion was associated with an extension of life span (49), which is consistent with the present findings (Fig. 1*G*). Similar results have been obtained in *Drosophila* and *Caenorhabditis elegans* (50–52). Furthermore, the results of a recent in vitro study indicated that relief from hyperexcitability and chronic, high intracellular Ca^{2+} concentration is important for the prevention of β-cell failure (53). Considering that a reduction in glucokinase expression could protect pancreatic β-cells from high intracellular Ca^{2+} in *db/db* mice, glucokinase inhibition could be expected to a new therapeutic strategy for β-cell rest in type 2 diabetes. The finding that glucokinase haploinsufficiency in β-cells of human islet amyloid polypeptide transgenic mice had a decreased incidence and quantity of islet amyloid (54) might demonstrate the usefulness of glucokinase inhibition.

Glucokinase inhibitors, including D-mannoheptulose, have been used as competitive antagonists to prevent glucose phosphorylation (33). However, there are challenges for clinical application. One is that the degree of glucokinase inhibition is important. Complete glucokinase inhibition would result in strong hyperglycemia, as shown in permanent neonatal diabetes mellitus with homozygous glucokinase-inactivating mutations (55). Another important point is the timing of glucokinase inhibition. Given that reduced numbers and/or function of pancreatic β-cells occurs even in the prediabetic state and are part of the natural history of type 2 diabetes progression (2–6), glucokinase inhibition could be more beneficial in individuals recently diagnosed with type 2 diabetes or prediabetes. Not all individuals with diabetes are eligible for this treatment strategy. More preclinical and clinical studies would determine the efficacy of glucokinase inhibition.

A limitation of the present study was that the mice were not pancreatic β-cell specific, although their hepatic expression of glucokinase was intact and their phenotype was very similar to that of β-cell–specific glucokinase knockout mice (9,56). β-Cell–specific knockout mice should be studied to confirm the present findings. On the other hand, it is unclear whether glucokinase inhibitors are pancreatic β-cell specific. Thus, it is necessary to explore the effect of glucokinase inhibition on the liver and brain.

In conclusion, glucokinase haploinsufficiency ameliorated glucose tolerance by insulin-secretion augmentation associated with the increase in β-cell mass in *db/db* mice. This finding proved that optimizing excess glucose signaling in β-cells by reducing glucokinase activity could prevent β-cell insufficiency due to excess glucose influx, leading to glucose tolerance improvement in diabetes status by preserving β-cell mass. Glucokinase inactivation in β-cells could be a potential strategy for the treatment of type 2 diabetes.

Acknowledgments. The authors thank Dr. Takashi Kadowaki and Dr. Naoto Kubota (Department of Diabetes and Metabolic Diseases, Graduate School of Medicine, University of Tokyo, Tokyo, Japan) for kindly providing the $Gck^{+/-}$ mice. The authors also thank Marika Watanabe, Natsumi Fujimori, and Yuiko Takeda (Department of Rheumatology, Endocrinology, and Nephrology, Faculty of Medicine and Graduate School of Medicine, Hokkaido University, Sapporo, Japan) for their excellent technical assistance and animal care. The authors thank Dr. Robert Blakytny, from Edanz Group (www.edanzediting.com/ac) for editing a draft of this manuscript.

Funding. This work was supported in part by Grants-in-Aid for Young Scientists (B) 26860683 and Scientific Research (C) 19K08992 from the Ministry of Education, Culture, Sports, Science and Technology of Japan; a Grant-in-Aid for the Translational Research program, Strategic PRomotion for practical application of INnovative medical Technology (TR-SPRINT), from the Japan Agency for Medical Research and Development; a Grant-in-Aid for Young Researchers from the Japan Association for Diabetes Education and Care; and Grants-in-Aid from the MSD Life Science Foundation, the Suzuken Memorial Foundation, the Akiyama Life Science Foundation, the Takeda Science Foundation, and the Suhara Memorial Foundation (to A.N.).

Duality of Interest. No potential conflicts of interest relevant to this article were reported.

Author Contributions. K.O., A.N., and Y.T. designed the studies. K.O., A.N., Y.Y., S.K., K.T., and N.K. performed the in vivo and ex vivo experiments. K.O., A.N., and H.N. analyzed data. K.O., A.N., H.M., H.K., K.Y.C., Y.T., and T.A. interpreted the data. K.O., A.N., and Y.T. drafted the manuscript. A.N. is a guarantor of this study and, as such, had full access to all the data in the study and takes responsibility for the integrity of the data and the accuracy of the data analysis.

Prior Presentation. Parts of this study were presented at the virtual 56th Annual Meeting of the European Association for the Study of Diabetes, 21–25 September 2020.

References

1. Saeedi P, Petersohn I, Salpea P, et al.; IDF Diabetes Atlas Committee. Global and regional diabetes prevalence estimates for 2019 and projections for 2030 and 2045: results from the *International Diabetes Federation Diabetes Atlas*, 9th edition. *Diabetes Res Clin Pract* 2019;157:107843
2. Butler AE, Janson J, Bonner-Weir S, Ritzel R, Rizza RA, Butler PC. Beta-cell deficit and increased beta-cell apoptosis in humans with type 2 diabetes. Diabetes 2003;52:102–110
3. Sakuraba H, Mizukami H, Yagihashi N, Wada R, Hanyu C, Yagihashi S. Reduced beta-cell mass and expression of oxidative stress-related DNA damage in the islet of Japanese type II diabetic patients. Diabetologia 2002;45:85–96
4. Rhodes CJ. Type 2 diabetes-a matter of beta-cell life and death? Science 2005;307:380–384
5. Prentki M, Nolan CJ. Islet beta cell failure in type 2 diabetes. J Clin Invest 2006;116:1802–1812
6. Hudish LI, Reusch JE, Sussel L. β Cell dysfunction during progression of metabolic syndrome to type 2 diabetes. J Clin Invest 2019;129:4001–4008
7. Vetere A, Choudhary A, Burns SM, Wagner BK. Targeting the pancreatic β-cell to treat diabetes. Nat Rev Drug Discov 2014;13:278–289
8. Matschinsky FM, Magnuson MA, Zelent D, et al. The network of glucokinase-expressing cells in glucose homeostasis and the potential of glucokinase activators for diabetes therapy. Diabetes 2006;55:1–12
9. Terauchi Y, Sakura H, Yasuda K, et al. Pancreatic beta-cell-specific targeted disruption of glucokinase gene. Diabetes mellitus due to defective insulin secretion to glucose. J Biol Chem 1995;270:30253–30256
10. Matschinsky FM. GKAs for diabetes therapy: why no clinically useful drug after two decades of trying? Trends Pharmacol Sci 2013;34:90–99
11. Nakamura A, Terauchi Y. Present status of clinical deployment of glucokinase activators. J Diabetes Investig 2015;6:124–132
12. Grimsby J, Sarabu R, Corbett WL, et al. Allosteric activators of glucokinase: potential role in diabetes therapy. Science 2003;301:370–373
13. Futamura M, Hosaka H, Kadotani A, et al. An allosteric activator of glucokinase impairs the interaction of glucokinase and glucokinase regulatory protein and regulates glucose metabolism. J Biol Chem 2006;281:37668–37674
14. Fyfe MC, White JR, Taylor A, et al. Glucokinase activator PSN-GK1 displays enhanced antihyperglycaemic and insulinotropic actions. Diabetologia 2007;50:1277–1287
15. Nakamura A, Shimazaki H, Ohyama S, Eiki J, Terauchi Y. Effect of long-term treatment with a small-molecule glucokinase activator on glucose metabolism, lipid profiles and hepatic function. J Diabetes Investig 2011;2:276–279
16. Futamura M, Yao J, Li X, et al. Chronic treatment with a glucokinase activator delays the onset of hyperglycaemia and preserves beta cell mass in the Zucker diabetic fatty rat. Diabetologia 2012;55:1071–1080
17. Nakamura A, Terauchi Y, Ohyama S, et al. Impact of small-molecule glucokinase activator on glucose metabolism and beta-cell mass. Endocrinology 2009;150:1147–1154
18. Nakamura A, Togashi Y, Orime K, et al. Control of beta cell function and proliferation in mice stimulated by small-molecule glucokinase activator under various conditions. Diabetologia 2012;55:1745–1754
19. Wei P, Shi M, Barnum S, Cho H, Carlson T, Fraser JD. Effects of glucokinase activators GKA50 and LY2121260 on proliferation and apoptosis in pancreatic INS-1 beta cells. Diabetologia 2009;52:2142–2150
20. Porat S, Weinberg-Corem N, Tornovsky-Babaey S, et al. Control of pancreatic β cell regeneration by glucose metabolism. Cell Metab 2011;13:440–449
21. Meininger GE, Scott R, Alba M, et al. Effects of MK-0941, a novel glucokinase activator, on glycemic control in insulin-treated patients with type 2 diabetes. Diabetes Care 2011;34:2560–2566
22. Wilding JP, Leonsson-Zachrisson M, Wessman C, Johnsson E. Dose-ranging study with the glucokinase activator AZD1656 in patients with type 2 diabetes mellitus on metformin. Diabetes Obes Metab 2013;15:750–759
23. Kiyosue A, Hayashi N, Komori H, Leonsson-Zachrisson M, Johnsson E. Dose-ranging study with the glucokinase activator AZD1656 as monotherapy in Japanese patients with type 2 diabetes mellitus. Diabetes Obes Metab 2013;15:923–930
24. Tornovsky-Babeay S, Dadon D, Ziv O, et al. Type 2 diabetes and congenital hyperinsulinism cause DNA double-strand breaks and p53 activity in β cells. Cell Metab 2014;19:109–121
25. Omori K, Nakamura A, Miyoshi H, et al. Effects of dapagliflozin and/or insulin glargine on beta cell mass and hepatic steatosis in db/db mice. Metabolism 2019;98:27–36
26. Junker BH, Klukas C, Schreiber F. VANTED: a system for advanced data analysis and visualization in the context of biological networks. BMC Bioinformatics 2006;7:109
27. Terauchi Y, Iwamoto K, Tamemoto H, et al. Development of non-insulin-dependent diabetes mellitus in the double knockout mice with disruption of insulin receptor substrate-1 and beta cell glucokinase genes. Genetic reconstitution of diabetes as a polygenic disease. J Clin Invest 1997;99:861–866
28. Terauchi Y, Takamoto I, Kubota N, et al. Glucokinase and IRS-2 are required for compensatory beta cell hyperplasia in response to high-fat diet-induced insulin resistance. J Clin Invest 2007;117:246–257
29. Guo S, Dai C, Guo M, et al. Inactivation of specific β cell transcription factors in type 2 diabetes. J Clin Invest 2013;123:3305–3316
30. Montemurro C, Nomoto H, Pei L, et al. IAPP toxicity activates HIF1α/PFKFB3 signaling delaying β-cell loss at the expense of β-cell function. Nat Commun 2019;10:2679
31. Haythorne E, Rohm M, van de Bunt M, et al. Diabetes causes marked inhibition of mitochondrial metabolism in pancreatic β-cells. Nat Commun 2019;10:2474
32. Corbin KL, Waters CD, Shaffer BK, Verrilli GM, Nunemaker CS. Islet hypersensitivity to glucose is associated with disrupted oscillations and increased impact of proinflammatory cytokines in islets from diabetes-prone male mice. Endocrinology 2016;157:1826–1838
33. Jahan I, Corbin KL, Bogart AM, et al. Reducing glucokinase activity restores endogenous pulsatility and enhances insulin secretion in islets from db/db mice. Endocrinology 2018;159:3747–3760
34. Dalbøge LS, Almholt DL, Neerup TS, et al. Characterisation of age-dependent beta cell dynamics in the male db/db mice. PLoS One 2013;8:e82813
35. Kjørholt C, Akerfeldt MC, Biden TJ, Laybutt DR. Chronic hyperglycemia, independent of plasma lipid levels, is sufficient for the loss of beta-cell differentiation and secretory function in the db/db mouse model of diabetes. Diabetes 2005;54:2755–2763
36. Shao J, Iwashita N, Ikeda F, et al. Beneficial effects of candesartan, an angiotensin II type 1 receptor blocker, on beta-cell function and morphology in db/db mice. Biochem Biophys Res Commun 2006;344:1224–1233
37. Harmon JS, Bogdani M, Parazzoli SD, et al. β-Cell-specific overexpression of glutathione peroxidase preserves intranuclear MafA and reverses diabetes in db/db mice. Endocrinology 2009;150:4855–4862
38. Kaneto H, Kajimoto Y, Miyagawa J, et al. Beneficial effects of antioxidants in diabetes: possible protection of pancreatic beta-cells against glucose toxicity. Diabetes 1999;48:2398–2406
39. Matsuoka TA, Kaneto H, Kawashima S, et al. Preserving Mafa expression in diabetic islet β-cells improves glycemic control in vivo. J Biol Chem 2015;290:7647–7657
40. Schisler JC, Fueger PT, Babu DA, et al. Stimulation of human and rat islet beta-cell proliferation with retention of function by the homeodomain transcription factor Nkx6.1. Mol Cell Biol 2008;28:3465–3476
41. Taylor BL, Liu FF, Sander M. Nkx6.1 is essential for maintaining the functional state of pancreatic beta cells. Cell Rep 2013;4:1262–1275
42. Xu J, Han J, Long YS, Epstein PN, Liu YQ. The role of pyruvate carboxylase in insulin secretion and proliferation in rat pancreatic beta cells. Diabetologia 2008;51:2022–2030

43. Li X, Cheng KKY, Liu Z, et al. The MDM2-p53-pyruvate carboxylase signalling axis couples mitochondrial metabolism to glucose-stimulated insulin secretion in pancreatic β-cells. Nat Commun 2016;7:11740
44. Osipovich AB, Stancill JS, Cartailler JP, Dudek KD, Magnuson MA. Excitotoxicity and overnutrition additively impair metabolic function and identity of pancreatic β-cells. Diabetes 2020;69:1476–1491
45. Stancill JS, Cartailler JP, Clayton HW, et al. Chronic β-cell depolarization impairs β-cell identity by disrupting a network of Ca^{2+}-regulated genes. Diabetes 2017;66:2175–2187
46. van Raalte DH, Verchere CB. Improving glycaemic control in type 2 diabetes: stimulate insulin secretion or provide beta-cell rest? Diabetes Obes Metab 2017; 19:1205–1213
47. Ma S, Viola R, Sui L, Cherubini V, Barbetti F, Egli D. β cell replacement after gene editing of a neonatal diabetes-causing mutation at the insulin locus. Stem Cell Reports 2018;11:1407–1415
48. Szabat M, Page MM, Panzhinskiy E, et al. Reduced insulin production relieves endoplasmic reticulum stress and induces β cell proliferation. Cell Metab 2016; 23:179–193
49. Templeman NM, Flibotte S, Chik JHL, et al. Reduced circulating insulin enhances insulin sensitivity in old mice and extends lifespan. Cell Rep 2017;20: 451–463
50. Broughton SJ, Piper MDW, Ikeya T, et al. Longer lifespan, altered metabolism, and stress resistance in *Drosophila* from ablation of cells making insulin-like ligands. Proc Natl Acad Sci U S A 2005;102:3105–3110
51. Broughton S, Alic N, Slack C, et al. Reduction of DILP2 in *Drosophila* triages a metabolic phenotype from lifespan revealing redundancy and compensation among DILPs. PLoS One 2008;3:e3721
52. Murphy CT, McCarroll SA, Bargmann CI, et al. Genes that act downstream of DAF-16 to influence the lifespan of *Caenorhabditis elegans*. Nature 2003;424: 277–283
53. Shyr ZA, Wang Z, York NW, Nichols CG, Remedi MS. The role of membrane excitability in pancreatic β-cell glucotoxicity. Sci Rep 2019;9:6952
54. Andrikopoulos S, Verchere CB, Terauchi Y, Kadowaki T, Kahn SE. Beta-cell glucokinase deficiency and hyperglycemia are associated with reduced islet amyloid deposition in a mouse model of type 2 diabetes. Diabetes 2000;49:2056–2062
55. Osbak KK, Colclough K, Saint-Martin C, et al. Update on mutations in glucokinase (GCK), which cause maturity-onset diabetes of the young, permanent neonatal diabetes, and hyperinsulinemic hypoglycemia. Hum Mutat 2009;30: 1512–1526
56. Terauchi Y, Kadowaki T. Insights into molecular pathogenesis of type 2 diabetes from knockout mouse models. Endocr J 2002;49:247–263